

Measurement of the Target-Normal Single-Spin Asymmetry in Quasi-Elastic Scattering from the Reaction ${}^3\text{He}^\uparrow(e, e')$

Y.-W. Zhang,^{1,2} E. Long,³ M. Mihovilović,⁴ G. Jin,⁵ K. Allada,⁶ B. Anderson,³ J. R. M. Annand,⁷ T. Averett,^{8,*} W. Boeglin,⁹ P. Bradshaw,⁸ A. Camsonne,⁶ M. Canan,¹⁰ G. D. Cates,⁵ C. Chen,¹¹ J. P. Chen,⁶ E. Chudakov,⁶ R. De Leo,¹² X. Deng,⁵ A. Deur,⁶ C. Dutta,¹³ L. El Fassi,¹ D. Flay,¹⁴ S. Frullani,¹⁵ F. Garibaldi,¹⁵ H. Gao,¹⁶ S. Gilad,¹⁷ R. Gilman,¹ O. Glamazdin,¹⁸ S. Golge,¹⁰ J. Gomez,⁶ O. Hansen,⁶ D. W. Higinbotham,⁶ T. Holmstrom,¹⁹ J. Huang,^{17,20} H. Ibrahim,²¹ C. W. de Jager,⁶ E. Jensen,²² X. Jiang,²⁰ J. St. John,¹⁹ M. Jones,⁶ H. Kang,²³ J. Katich,⁸ H. P. Khanal,⁹ P. King,²⁴ W. Korsch,¹³ J. LeRose,⁶ R. Lindgren,⁵ H.-J. Lu,²⁵ W. Luo,²⁶ P. Markowitz,⁹ M. Meziane,⁸ R. Michaels,⁶ B. Moffit,⁶ P. Monaghan,¹¹ N. Muangma,¹⁷ S. Nanda,⁶ B. E. Norum,⁵ K. Pan,¹⁷ D. Parno,²⁷ E. Piassetzky,²⁸ M. Posik,¹⁴ V. Punjabi,²⁹ A. J. R. Puckett,²⁰ X. Qian,¹⁶ Y. Qiang,⁶ X. Qiu,²⁶ S. Riordan,⁵ G. Ron,³⁰ A. Saha,^{6,†} B. Sawatzky,⁶ R. Schiavilla,^{6,10} B. Schoenrock,³¹ M. Shabestari,⁵ A. Shahinyan,³² S. Širca,^{33,4} R. Subedi,³⁴ V. Sulkosy,¹⁷ W. A. Tobias,⁵ W. Tireman,³¹ G. M. Urciuoli,¹⁵ D. Wang,⁵ K. Wang,⁵ Y. Wang,³⁵ J. Watson,⁶ B. Wojtsekhowski,⁶ Y. Ye,³⁶ Z. Ye,¹¹ X. Zhan,¹⁷ Y. Zhang,²⁶ X. Zheng,⁵ B. Zhao,⁸ and L. Zhu¹¹

(The Jefferson Lab Hall A Collaboration)

¹Rutgers University, New Brunswick, NJ 08901, USA

²University of Pennsylvania, Philadelphia, PA, 19104, USA

³Kent State University, Kent, OH 44242, USA

⁴Jožef Stefan Institute, SI-1000 Ljubljana, Slovenia

⁵University of Virginia, Charlottesville, VA 22908, USA

⁶Thomas Jefferson National Accelerator Facility, Newport News, VA 23606, USA

⁷Glasgow University, Glasgow G12 8QQ, Scotland, United Kingdom

⁸The College of William and Mary, Williamsburg, VA 23187, USA

⁹Florida International University, Miami, FL 33181, USA

¹⁰Old Dominion University, Norfolk, VA 23529, USA

¹¹Hampton University, Hampton, VA 23669, USA

¹²Università degli studi di Bari Aldo Moro, I-70121 Bari, Italy

¹³University of Kentucky, Lexington, KY 40506, USA

¹⁴Temple University, Philadelphia, PA 19122, USA

¹⁵Istituto Nazionale Di Fisica Nucleare, INFN/Sanita, Roma, Italy

¹⁶Duke University, Durham, NC 27708, USA

¹⁷Massachusetts Institute of Technology, Cambridge, MA 02139, USA

¹⁸Kharkov Institute of Physics and Technology, Kharkov 61108, Ukraine

¹⁹Longwood University, Farmville, VA 23909, USA

²⁰Los Alamos National Laboratory, Los Alamos, NM 87545, USA

²¹Cairo University, Cairo, Giza 12613, Egypt

²²Christopher Newport University, Newport News VA 23606, USA

²³Seoul National University, Seoul, Korea

²⁴Ohio University, Athens, OH 45701, USA

²⁵Huangshan University, People's Republic of China

²⁶Lanzhou University, Lanzhou, Gansu, 730000, People's Republic of China

²⁷Carnegie Mellon University, Pittsburgh, PA 15213, USA

²⁸Tel Aviv University, Tel Aviv 69978, Israel

²⁹Norfolk State University, Norfolk, VA 23504, USA

³⁰Hebrew University of Jerusalem, Jerusalem 91904 Israel

³¹Northern Michigan University, Marquette, MI 49855, USA

³²Yerevan Physics Institute, Yerevan, Armenia

³³University of Ljubljana, SI-1000 Ljubljana, Slovenia

³⁴George Washington University, Washington, D.C. 20052, USA

³⁵University of Illinois at Urbana-Champaign, Urbana, IL 61801, USA

³⁶University of Science and Technology, Hefei, People's Republic of China

(Dated: February 10, 2015)

We report the first measurement of the target single-spin asymmetry, A_y , in quasi-elastic scattering from the inclusive reaction ${}^3\text{He}^\uparrow(e, e')$ on a ${}^3\text{He}$ gas target polarized normal to the lepton scattering plane. Assuming time-reversal invariance, this asymmetry is strictly zero for one-photon exchange. A non-zero A_y can arise from the interference between the one- and two-photon exchange processes which is sensitive to the details of the sub-structure of the nucleon. An experiment recently completed at Jefferson Lab yielded asymmetries with high statistical precision at $Q^2 = 0.13, 0.46$ and 0.97 GeV^2 . These measurements demonstrate, for the first time, that the ${}^3\text{He}$ asymmetry

is clearly non-zero and negative with a statistical significance of $(8-10)\sigma$. Using measured proton-to- ^3He cross-section ratios and the effective polarization approximation, neutron asymmetries of $-(1-3)\%$ were obtained. The neutron asymmetry at high Q^2 is related to moments of the Generalized Parton Distributions (GPDs). Our measured neutron asymmetry at $Q^2 = 0.97 \text{ GeV}^2$ agrees well with a prediction based on two-photon exchange using a GPD model and thus provides a new, independent constraint on these distributions.

PACS numbers: 24.70.+s, 14.20.Dh, 29.25.Pj

Elastic and inelastic form factors, extracted from electron-nucleon scattering data, provide invaluable information on nucleon structure. In most cases the scattering cross sections are dominated by one-photon exchange. Contributions from two-photon exchange are suppressed relative to the one-photon exchange contribution but are important in certain processes.

One observable that is exactly zero for one-photon exchange is the target-normal single-spin asymmetry (SSA), A_y , which is the focus of this experiment. When two-photon exchange is included, A_y can be non-zero. As shown in Fig. 1 the two photons form a loop that contains the nucleon intermediate state which has an elastic contribution that is calculable [1], and an inelastic contribution that must be modeled. This makes the two-photon exchange process sensitive to the details of nucleon structure and provides a powerful new tool for testing model predictions.

Recently, A_y for the neutron (^3He) was measured to be non-zero and negative at the 2.89σ level for deep-inelastic scattering [2]. Two-photon-exchange contributions are also important when extracting the proton elastic form factor $G_E^p(Q^2)$ from measured data. Values extracted from Rosenbluth separation of cross section data differ markedly from those extracted from polarization-transfer measurements [1, 3–7]. A GPD-based model prediction for the two-photon exchange contributions reduced the discrepancy by $\sim 50\%$ for $Q^2 \geq 1 \text{ GeV}^2$ [1]. This same model also predicts $A_y \sim -2\%$ at $Q^2 = 1 \text{ GeV}^2$. A measurement of A_y is thus an independent test of the GPD model in the absence of a large contribution from one-photon exchange.

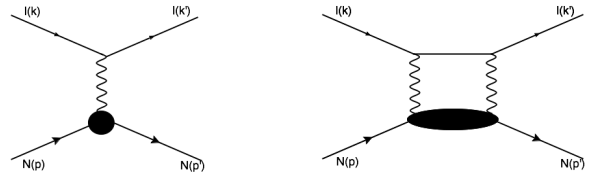


FIG. 1. In inclusive electron scattering a non-zero target-normal SSA can arise due to interference between one- (left) and two- (right) photon exchange. Here N is the nucleon with incident and outgoing 4-momenta p and p' , respectively, and l is the lepton with incident and outgoing 4-momenta k and k' , respectively. The intermediate nucleon state, represented by the black oval, includes both elastic and inelastic contributions and is thus sensitive to the structure of the nucleon.

Consider the elastic scattering of an unpolarized electron from a target nucleon with spin \vec{S} , oriented perpendicular (transversely polarized) to the incident electron 3-momentum \vec{k} , and normalized such that $|\vec{S}| = 1$. Requiring conservation of both the electromagnetic current and parity, the differential cross section, $d\sigma$, for the inclusive (e, e') reaction is written as [8–10]

$$\begin{aligned} d\sigma(\phi_S) &= d\sigma_{UU} + \frac{\vec{S} \cdot (\vec{k} \times \vec{k}')}{|\vec{k} \times \vec{k}'|} d\sigma_{UT} \\ &= d\sigma_{UU} + d\sigma_{UT} \sin \phi_S, \end{aligned} \quad (1)$$

where \vec{k}' is the 3-momentum of the scattered electron, and $d\sigma_{UU}$ and $d\sigma_{UT}$ are the cross sections for an unpolarized electron scattered from an unpolarized and transversely polarized target, respectively. Our choice of coordinates is shown in Fig. 2 with the angle ϕ_S between the lepton plane and \vec{S} . The $+\hat{y}$ direction is parallel to the vector $\vec{k} \times \vec{k}'$ and corresponds to $\phi_S = 90^\circ$. We define the target SSA as

$$A_{UT}(\phi_S) = \frac{d\sigma(\phi_S) - d\sigma(\phi_S + \pi)}{d\sigma(\phi_S) + d\sigma(\phi_S + \pi)} = A_y \sin \phi_S. \quad (2)$$

By measuring A_{UT} at $\phi_S = \pi/2$ one can extract the quantity $A_y \equiv \frac{d\sigma_{UT}}{d\sigma_{UU}}$, which is the SSA for a target polarized normal to the lepton plane.

For one-photon exchange we can write $d\sigma_{UU} \propto \text{Re}(\mathcal{M}_{1\gamma}\mathcal{M}_{1\gamma}^*)$ and $d\sigma_{UT} \propto \text{Im}(\mathcal{M}_{1\gamma}\mathcal{M}_{1\gamma}^*)$, where $\mathcal{M}_{1\gamma}$ is the one-photon exchange amplitude and Re (Im) stands for the real (imaginary) part. However, time-reversal invariance requires that $\mathcal{M}_{1\gamma}$ be real and so at order α^2 , $d\sigma_{UU}$ can be non-zero, but $d\sigma_{UT}$ must be zero [8]. When one includes the (complex) two-photon exchange amplitude, $\mathcal{M}_{2\gamma}$, the contribution to the asymmetry from the

* Corresponding author: tdaver@wm.edu

† Deceased.

interference between one- and two-photon exchange amplitudes is $d\sigma_{UT} \propto \text{Im}(\mathcal{M}_{1\gamma}\mathcal{M}_{2\gamma}^*)$ which can be non-zero at order α^3 .

Using the formalism of Ref. [1], we can write

$$A_y = \sqrt{\frac{2\varepsilon(1+\varepsilon)}{\tau}} \frac{1}{\sigma_R} \left\{ -G_M \text{Im} \left(\delta\tilde{G}_E + \frac{\nu}{M^2} \tilde{F}_3 \right) + G_E \text{Im} \left(\delta\tilde{G}_M + \left(\frac{2\varepsilon}{1+\varepsilon} \right) \frac{\nu}{M^2} \tilde{F}_3 \right) \right\}, \quad (3)$$

where $\tau \equiv Q^2/4M^2$, $\nu = \frac{1}{4}(k_\mu + k'_\mu)(p^\mu + p'^\mu)$, $\varepsilon \equiv (1 + 2(1 + \tau) \tan^2 \frac{\theta}{2})^{-1}$ and M is the mass of the nucleon. In the lab frame, E , E' and θ are the incident and scattered energies, and scattering angle, of the electron, respectively. The G_E and G_M are the Sachs form factors and σ_R is the unpolarized cross section. The terms $\delta\tilde{G}_E$, $\delta\tilde{G}_M$ and \tilde{F}_3 are additional complex contributions that arise when two-photon exchange is included. They are exactly zero for one-photon exchange. For the neutron, unlike the proton, $G_E \ll G_M$ so that Eq. (3) is dominated by the term proportional to G_M . Note that the unpolarized cross section and polarization transfer observables depend on the real parts of $\delta\tilde{G}_E$, $\delta\tilde{G}_M$ and \tilde{F}_3 .

For $Q^2 \geq 1 \text{ GeV}^2$ the two-photon contributions to Eq. (3) were estimated using weighted moments of the GPDs, H^q , E^q and \tilde{H}^q , for a quark q [1]. For lower Q^2 , A_y can be estimated using model fits of nucleon resonance and pion production data [6, 11]. However, there are no predictions in the kinematic range of this experiment. The only existing measurement was made on the proton at SLAC in 1970 [12]. They measured asymmetries at $Q^2 = 0.38, 0.59$ and 0.98 GeV^2 that were consistent with zero at the $\sim 10^{-2}$ level. There has never been a corresponding measurement on the neutron.

This paper presents the results of Jefferson Lab experiment E05-015, which measured A_y by scattering unpolarized electrons from ^3He nuclei polarized normal to the electron scattering plane. The electron beam was longitudinally polarized with energies of 1.2, 2.4 and 3.6 GeV and an average current of $12 \mu\text{A}$ (CW). The helicity of the beam was flipped at a rate of 30 Hz (for other experiments requiring a polarized electron beam) and data from the two helicity states were summed for this analysis.

The polarized target used in this experiment was a 40 cm-long aluminosilicate glass cell filled with ^3He gas at a density of 10.9 amg. A small quantity of N_2 gas, ~ 0.1 amg, was also included to aid in the polarization process. The target was polarized through spin-exchange optical pumping of a Rb-K mixture [16]. In order to reduce the systematic uncertainty, the direction of the target polarization vector was reversed every 20 minutes using adiabatic fast passage. The polarization was monitored during each spin-flip using nuclear magnetic resonance. Electron paramagnetic resonance measurements were periodically made throughout the experiment in order to

calibrate the polarization [17]. The average in-beam target polarization was $(51.4 \pm 2.9)\%$.

The electron beam was rastered in a $3 \text{ mm} \times 3 \text{ mm}$ pattern to reduce the possibility of cell rupture due to localized heating of the thin glass windows. Electrons scattered from the target were detected using the two Hall A high resolution spectrometers (HRSEs) [18] at scattering angles of $\pm 17^\circ$ with respect to the incident beam direction. Both spectrometers were configured to detect electrons in single-arm mode using nearly identical detector packages, each consisting of two dual-plane vertical drift chambers for tracking, two planes of segmented plastic scintillator for trigger formation, and CO_2 gas Cherenkov and Pb-glass electromagnetic calorimeter detectors for hadron rejection. The data acquisition systems for the spectrometers were synchronized to allow cross-checking of the results. By simultaneously measuring with two independent spectrometers, we confirmed that the measured asymmetries were consistent in magnitude, with opposite signs, as expected.

Consistent with Ref. [2], the lepton scattering plane is defined by the incoming and outgoing electron momenta, \vec{k} and \vec{k}' , respectively, as in Figure 2. If the target spin is parallel to \hat{y} , we define it as spin up (\uparrow), while the target spin is anti-parallel to \hat{y} is defined as spin down (\downarrow).

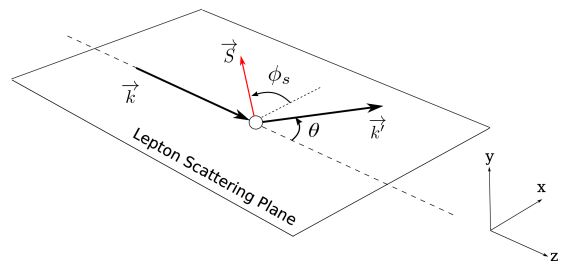


FIG. 2. Coordinate system used to define $A_{UT}(\phi_s)$.

The electron yields, $Y^{\uparrow(\downarrow)}$, give the number of electrons ($N^{\uparrow(\downarrow)}$) in the target spin-up (spin-down) state that pass all the particle-identification cuts, normalized by accumulated charge ($Q^{\uparrow(\downarrow)}$) and data-acquisition live-time ($LT^{\uparrow(\downarrow)}$):

$$Y^{\uparrow(\downarrow)} = \frac{N^{\uparrow(\downarrow)}}{Q^{\uparrow(\downarrow)} \cdot LT^{\uparrow(\downarrow)}} \quad (4)$$

The raw experimental asymmetries were calculated as

$$A_{\text{raw}} = \frac{Y^{\uparrow} - Y^{\downarrow}}{Y^{\uparrow} + Y^{\downarrow}} \quad (5)$$

and were corrected for nitrogen dilution and target polarization. The nitrogen dilution factor is defined as

$$f_{\text{N}_2} \equiv \frac{\rho_{\text{N}_2} \sigma_{\text{N}_2}}{\rho_{^3\text{He}} \sigma_{^3\text{He}} + \rho_{\text{N}_2} \sigma_{\text{N}_2}}, \quad (6)$$

where ρ_i and σ_i are the number densities and unpolarized cross sections, respectively. The nitrogen density was

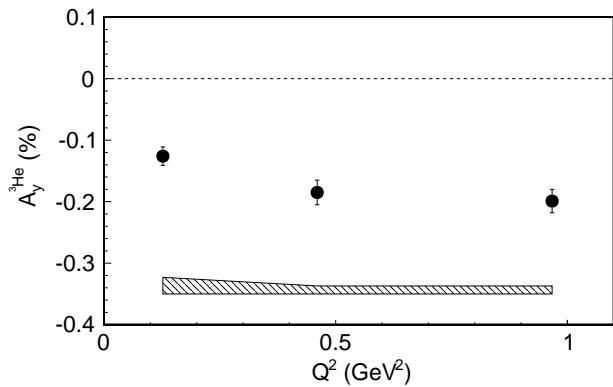


FIG. 3. Measured ${}^3\text{He}$ asymmetries, $A_y^{3\text{He}}$, as a function of Q^2 . Uncertainties shown on the data points are statistical. Systematic uncertainties are shown by the band at the bottom.

measured when filling the target cell and the cross-section was determined experimentally by electrons scattering from a reference cell filled with a known quantity of N_2 . The denominator was obtained from the polarized target cell yields.

The final asymmetries were obtained after subtraction of the elastic radiative tail contribution, radiative corrections of the quasi-elastic asymmetries and corrections for bin-averaging effects. The contribution of the elastic radiative tail to the lowest Q^2 point was 3%, and was negligible for the two larger Q^2 points. Results for $A_y^{3\text{He}}$ are shown in Fig. 3 and listed in Table I. The uncertainties on the data points are statistical, with the total experimental systematic uncertainty indicated as an error band below the data points. The systematic uncertainty in $A_y^{3\text{He}}$ includes contributions from the live-time asymmetry, target polarization, target misalignment, nitrogen dilution and radiative corrections. The dominant contribution to the systematic uncertainty at the two largest Q^2 points is the uncertainty in the target polarization, $\pm 5.6\%$ (rel.). At the two largest Q^2 points, the results from the left and right HRS agree to $< 1\sigma$ (stat.). At the lowest Q^2 point the results differ by $\sim 2\sigma$ (stat.), which we included in the systematic uncertainty.

Polarized ${}^3\text{He}$ targets have been used in many experiments as an effective polarized neutron target [13, 14]. The ground state of the ${}^3\text{He}$ nucleus is dominated by the S -state in which the two proton spins are anti-parallel, and the nuclear spin is carried by the neutron [15]. From the polarized ${}^3\text{He}$ asymmetries, the neutron asymmetries, A_y^n , were extracted using the effective neutron polarization approximation [19],

$$A_y^n = \frac{1}{(1 - f_p)P_n} (A_y^{3\text{He}} - f_p P_p A_y^p) \quad (7)$$

where the proton dilution factors, f_p , were calculated using the Kelly parametrizations for G_E^p and G_M^p [20] and

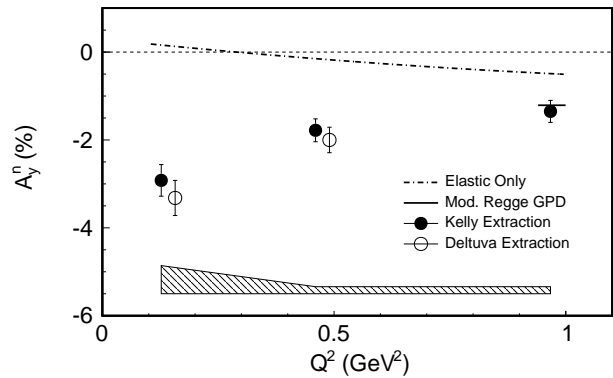


FIG. 4. Results for the neutron asymmetries, A_y^n , as a function of Q^2 . Uncertainties shown on the data points are statistical. Systematic uncertainties are shown by the band at the bottom. The elastic contribution to the intermediate state is shown by the dot-dash line [26], and at $Q^2 = 0.97$ GeV^2 , the GPD calculation of Chen *et al.* [1] is shown by the short solid line.

assuming $f_p = (1 - f_n) = 2\sigma_p/\sigma_{3\text{He}} = 2\sigma_p/(2\sigma_p + \sigma_n)$. At the lowest two Q^2 points, where nuclear effects may be important, a calculation was also made by A. Deltuva [21–24] using a non-relativistic model of the ${}^3\text{He}$ nucleus based on the CD-Bonn potential. Results extracted using the Kelly and Deltuva methods are consistent.

The effective neutron and proton polarizations in ${}^3\text{He}$ are given by $P_n = 0.86_{-0.02}^{+0.036}$ and $P_p = -0.028_{-0.004}^{+0.009}$ [25], respectively. The proton asymmetries, A_y^p , were predicted to be 0.01%, 0.24% and 0.62% for $Q^2 = 0.13, 0.46$ and 0.97 GeV^2 , respectively, using an estimate of the elastic intermediate state contribution in lieu of precision data [26]. The contribution from A_y^p is suppressed by the small effective proton polarization in polarized ${}^3\text{He}$. The neutron single-spin asymmetries calculated using Eq. (7) are shown in Fig. 4 and listed in Table I along with values for f_n .

In summary, we have reported the first measurement of the target single-spin asymmetries, A_y , from quasi-elastic (e, e') scattering from a ${}^3\text{He}$ target polarized normal to the electron scattering plane. This measurement demonstrates, for the first time, that the ${}^3\text{He}$ asymmetries are clearly non-zero and negative with a statistical significance of $(8 - 10)\sigma$. Neutron asymmetries were extracted using the effective neutron polarization approximation and are also clearly non-zero and negative. The results are inconsistent with an estimate where only the elastic intermediate state is included [26] but are consistent with a model using GPD input for the inelastic intermediate state contribution at $Q^2 = 0.97$ GeV^2 [1].

We acknowledge the outstanding support of the Jefferson Lab Hall A technical staff and Accelerator Division in accomplishing this experiment. We wish to thank Profs. A. Deltuva, Univ. de Lisboa, A. Afanasev, Jefferson Lab and M. Vanderhaeghen, MAINZ, for theoretical

guidance and calculations. This work was supported in part by the U.S. National Science Foundation, the U.S. Department of Energy and by DOE contract DE-AC05-06OR23177, under which Jefferson Science Associates,

LLC operates the Thomas Jefferson National Accelerator Facility, the National Science Foundation of China and UK STFC grants 57071/1, 50727/1.

-
- [1] Y. Chen, A. Afanasev, S. Brodsky, C. Carlson, and M. Vanderhaeghen, *Phys.Rev.Lett.* **93**, 122301 (2004).
- [2] J. Katich, X. Qian, Y. Zhao, K. Allada, K. Aniol, *et al.*, *Phys.Rev.Lett.* **113**, 022502 (2014), arXiv:1311.0197 [nucl-ex].
- [3] J. Arrington, *Phys. Rev. C* **68**, 034325 (2003).
- [4] J. Arrington, P. Blunden, and W. Melnitchouk, *Prog.Part.Nucl.Phys.* **66**, 782 (2011), arXiv:1105.0951 [nucl-th].
- [5] A. Puckett, E. Brash, O. Gayou, M. Jones, L. Pentchev, *et al.*, *Phys.Rev.* **C85**, 045203 (2012).
- [6] P. G. Blunden, W. Melnitchouk, and J. A. Tjon, *Phys. Rev. Lett.* **91**, 142304 (2003).
- [7] C. E. Carlson and M. Vanderhaeghen, *Annu. Rev. Nucl. Part. Sci.* **57**, 171 (2007).
- [8] N. Christ and T. D. Lee, *Phys. Rev.* **143**, 1310 (1966).
- [9] R. N. Cahn and Y. S. Tsai, *Phys. Rev.* **D2**, 870 (1970).
- [10] A. Afanasev, M. Strikman, and C. Weiss, *Phys. Rev.* **D77**, 014028 (2008).
- [11] B. Pasquini and M. Vanderhaeghen, *Phys.Rev.* **C70**, 045206 (2004), arXiv:hep-ph/0405303 [hep-ph].
- [12] T. Powell, M. Borghini, O. Chamberlain, R. Z. Fuzesy, C. C. Morehouse, *et al.*, *Phys.Rev.Lett.* **24**, 753 (1970).
- [13] S. Kuhn, J.-P. Chen, and E. Leader, *Prog.Part.Nucl.Phys.* **63**, 1 (2009), arXiv:0812.3535 [hep-ph].
- [14] X. Qian *et al.* (Jefferson Lab Hall A Collaboration), *Phys.Rev.Lett.* **107**, 072003 (2011), arXiv:1106.0363 [nucl-ex].
- [15] F. Bissey, V. Guzey, M. Strikman, and A. Thomas, *Phys. Rev. C* **65**, 064317 (2002).
- [16] J. Singh, P. Dolph, W. Tobias, T. Averett, A. Kelleher, *et al.*, (2013), arXiv:1309.4004 [physics.atom-ph].
- [17] M. V. Romalis and G. D. Cates, *Phys. Rev. A* **58**, 3004 (1998).
- [18] J. Alcorn, B. Anderson, K. Aniol, J. Annand, L. Auerbach, *et al.*, *Nucl.Instrum.Meth.* **A522**, 294 (2004).
- [19] S. Scopetta, *Phys. Rev. D* **75**, 054005 (2007).
- [20] J. J. Kelly, *Phys. Rev. C* **70**, 068202 (2004).
- [21] A. Deltuva, R. Machleidt, and P. Sauer, *Phys. Rev. C* **68**, 024005 (2003).
- [22] A. Deltuva, L. Yuan, J. Adam, A. Fonseca, and P. Sauer, *Phys. Rev. C* **69**, 034004 (2004).
- [23] A. Deltuva, L. Yuan, J. Adam, and P. Sauer, *Phys. Rev. C* **70**, 034004 (2004).
- [24] A. Deltuva, A. Fonseca, and P. Sauer, *Phys. Rev. C* **72**, 054004 (2005).
- [25] X. Zheng *et al.* (Jefferson Lab Hall A Collaboration), *Phys. Rev. Lett.* **92**, 012004 (2004).
- [26] A. Afanasev, I. Akushevich, and N. Merenkov, (2002), arXiv:hep-ph/0208260 [hep-ph].

E (GeV)	$\langle E' \rangle$ (GeV)	$\langle \theta \rangle$ deg.	$\langle Q^2 \rangle$ (GeV ²)	$A_y^{3\text{He}}$ (%)	f_n (Kelly)	A_y^n (%) (Kelly)	f_n (Deltuva)	A_y^n (%) (Deltuva)
1.245	1.167	17.0	0.127	$-0.126 \pm 0.015 \pm 0.027$	0.050	$-2.92 \pm 0.36 \pm 0.64$	0.044	$-3.32 \pm 0.40 \pm 0.72$
2.425	2.170	17.0	0.460	$-0.185 \pm 0.020 \pm 0.013$	0.117	$-1.78 \pm 0.26 \pm 0.16$	0.104	$-2.00 \pm 0.29 \pm 0.18$
3.605	3.070	17.0	0.967	$-0.199 \pm 0.019 \pm 0.013$	0.159	$-1.35 \pm 0.25 \pm 0.16$	-	-

TABLE I. Measured ^3He asymmetries, $A_y^{3\text{He}}$ (%). Neutron dilution factors, f_n , and asymmetries, A_y^n , were extracted using the Deltuva and Kelly models for ^3He . Uncertainties are statistical and systematic, respectively.